



ORIGINAL RESEARCH

Immunoprofiling of *Drosophila* Hemocytes by Single-cell Mass Cytometry



József Á. Balog^{1,2,#}, Viktor Honti^{3,#}, Éva Kurucz^{3,#}, Beáta Kari³,
 László G. Puskás¹, István Andó^{3,*},§, Gábor J. Szébeni^{1,4,*},§

¹ Laboratory of Functional Genomics, Institute of Genetics, Biological Research Centre, Szeged H-6726, Hungary

² University of Szeged, Ph.D. School in Biology, Szeged H-6726, Hungary

³ Immunology Unit, Institute of Genetics, Biological Research Centre, Szeged H-6726, Hungary

⁴ Department of Physiology, Anatomy and Neuroscience, Faculty of Science and Informatics, University of Szeged, Szeged H-6726, Hungary

Received 14 November 2019; revised 11 June 2020; accepted 28 June 2020

Available online 10 March 2021

Handled by Rong Fan

KEYWORDS

Mass cytometry;
 Innate immunity;
Drosophila;
 Single-cell analysis;
 Hemocyte

Abstract Single-cell mass cytometry (SCMC) combines features of traditional flow cytometry (*i.e.*, fluorescence-activated cell sorting) with mass spectrometry, making it possible to measure several parameters at the single-cell level for a complex analysis of biological regulatory mechanisms. In this study, we optimized SCMC to analyze **hemocytes** of the *Drosophila* innate immune system. We used metal-conjugated antibodies (against cell surface antigens H2, H3, H18, L1, L4, and P1, and intracellular antigens 3A5 and L2) and anti-IgM (against cell surface antigen L6) to detect the levels of antigens, while anti-GFP was used to detect crystal cells in the immune-induced samples. We investigated the antigen expression profile of single cells and hemocyte populations in naive states, in immune-induced states, in tumorous mutants bearing a driver mutation in the *Drosophila* homologue of Janus kinase (*hop^{Tum}*) and carrying a deficiency of the tumor suppressor gene *lethal(3)malignant blood neoplasm-1* [*l(3)mbn¹*], as well as in stem cell maintenance-defective *hdc^{Δ84}* mutant larvae. Multidimensional analysis enabled the discrimination of the functionally different major hemocyte subsets for lamellocytes, plasmatocytes, and crystal cells, and delineated the unique immunophenotype of *Drosophila* mutants. We have identified subpopulations of L2⁺/P1⁺ and L2⁺/L4⁺/P1⁺ transitional phenotype cells in the tumorous strains *l(3)mbn¹* and *hop^{Tum}*, respectively, and a subpopulation of L4⁺/P1⁺ cells upon immune induction. Our results

* Corresponding authors.

E-mail: ando@brc.hu (Andó I), szebeni.gabor@brc.hu (Szébeni GJ).

Equal contribution.

§ Current address: Institute of Genetics, Biological Research Centre, Szeged H-6726, Hungary.

Peer review under responsibility of Beijing Institute of Genomics, Chinese Academy of Sciences / China National Center for Bioinformation and Genetics Society of China.

<https://doi.org/10.1016/j.gpb.2020.06.022>

1672-0229 © 2021 The Authors. Published by Elsevier B.V. and Science Press on behalf of Beijing Institute of Genomics, Chinese Academy of Sciences / China National Center for Bioinformation and Genetics Society of China.

This is an open access article under the CC BY-NC-ND license (<http://creativecommons.org/licenses/by-nc-nd/4.0/>).

demonstrated for the first time that SCMC, combined with multidimensional bioinformatic analysis, represents a versatile and powerful tool to deeply analyze the regulation of cell-mediated immunity of *Drosophila*.

Introduction

In the animal kingdom, insects have multi-layered innate immune defense mechanisms against invading pathogens. Investigation on insects, including the fruit fly *Drosophila melanogaster* that lacks an acquired immune response, plays an important role in our understanding of how innate immunity works [1,2]. The conserved signaling pathways between insects and vertebrates, combined with the powerful genetic resources of *Drosophila*, make *Drosophila* an ideal system to model biological phenomena related to human biology and medicine. In *Drosophila*, microbial infection induces a powerful humoral immune response, *i.e.*, release of antimicrobial peptides, the regulation of which is now well understood [3]. Parasite infection, wounding, or tumorous development induces a cellular immune response by blood cells, *i.e.*, the hemocytes. Recognition, encapsulation, and killing of parasites, or phagocytosis of microorganisms [4–6] is exerted by specialized blood cells, *i.e.*, the phagocytic plasmatocytes, the encapsulating lamellocytes, and the melanizing crystal cells. Quantitative methods are developed to identify mechanisms underlying cell-mediated immunity in *Drosophila*, and these mechanistic studies facilitate further investigations or manipulations of immune cells and tissues. In addition, transgenic reporter constructs and monoclonal antibodies have also been developed to define functional hemocyte subsets. These systems generally use fluorescent molecules in the form of *in vivo* markers or antibodies, which significantly contribute to our understanding of innate immunity [7–9].

Recently, single-cell mass cytometry (SCMC) was developed to monitor the expression of marker molecules in hematological and other pathological conditions [10,11]. Antibodies against cell type-specific antigens can be applied to monitor blood cell differentiation during ontogenesis or following immune induction. However, traditional antibody staining against only one or two of the cell type-specific antigens is not sufficient to describe individual hemocyte populations with complex antigen expression patterns. Therefore, we adopted and optimized SCMC for *Drosophila* by multiplex analysis of antibodies to transmembrane proteins or intracellular antigens of IgG and IgM types, which are routinely used for detecting and discriminating hemocyte subsets of *Drosophila melanogaster* [7,12–16].

The circulating hemocytes of the *Drosophila* larvae are classified into three categories. Two cell types are present only in naive condition. These include the small round phagocytic plasmatocytes, which account for 95% of the circulating hemocytes, and the melanizing crystal cells, which are similar in size to plasmatocytes but contain prophenoloxidase crystals in their cytoplasm. The third cell type is the large flattened lamellocytes, which differentiate only in tumorous larvae and in case of immune induction, such as wounding or parasitic wasp infestation [17]. Lamellocytes, together with plasmatocytes, are capable of forming a multilayer capsule around the wasp egg, thereby killing the invader [18–20]. Plasmatocytes, crystal cells, and lamellocytes can be distinguished using cell

type-specific monoclonal antibodies or *in vivo* transgenic reporters [7–9,12–15]. All plasmatocytes express P1 antigen (encoded by *nimC1*) [21], while lamellocytes show a characteristic expression of L1 (encoded by *atilla*), L2, L4, and L6 antigens [14]. Following immune induction, a portion of plasmatocytes transdifferentiate into lamellocytes to fight the parasitic wasp egg [22–25]. This transdifferentiation process is accompanied by a stepwise alteration of lamellocyte-specific antigen expression.

Understanding cancer remains a challenge for scientists. The conserved signal transduction pathways in *Drosophila* and the easy genetic manipulation make *Drosophila* a frequently used model organism to study cancer [26]. Therefore, we investigated two different tumorous *Drosophila* strains. One strain bears a driver mutation (*hop^{Tum}*) in the *hopscotch* (*hop*) gene encoding a Janus kinase, and the other strain carries a deficiency of the tumor suppressor gene *lethal(3)malignant blood neoplasm-1* [*l(3)mbn-1*], which is named as *l(3)mbn¹*. Constitutive activation of Hop causes melanotic tumors and lymph gland hypertrophy in the larvae, as well as malignant neoplasia of blood cells in *hop^{Tum}* *Drosophila* [27]. The homozygous mutation of *l(3)mbn¹* causes malignant transformation, enhanced hemocyte proliferation, and lamellocyte differentiation of blood cells in *l(3)mbn¹* *Drosophila* [28]. We also investigated the immunophenotype of a strain carrying a mutation in *hdc* (*hdc^{As4}*), which encodes Headcase, a *Drosophila* homolog of the human tumor suppressor Headcase protein homolog (HECA), and plays a role in hematopoietic stem cell maintenance [29,30]. In addition, *Oregon-R* (*Ore-R*) and *white* (*w¹¹¹⁸*) were included as reference strains, since they were previously considered as wild type and used for the generation of mutants [31]. Immune activation was monitored successfully by infestation with the *Leptopilina boulardi* parasitoid wasp of *Drosophila* larvae in the *lozenge>GFP* strain (*lz>GFP; lz-Gal4, UAS-GFP; +; +*), in which crystal cells were monitored by metal tag-labeled anti-GFP antibody [32,33].

We are the first to demonstrate that SCMC is a powerful tool for characterizing hemocytes in different *Drosophila* mutant strains at the protein level. Bioinformatic analysis revealed the characteristic protein expression pattern of hemocyte subsets at the single-cell resolution from different genetic variants examined. These together suggest that SCMC is a valuable tool for characterizing immune phenotypes in any model organisms, in which antibodies against immune components are available.

Results and discussion

SCMC reveals transitional phenotypes of hemocytes in the tumorous *hop^{Tum}* and *l(3)mbn¹* strains

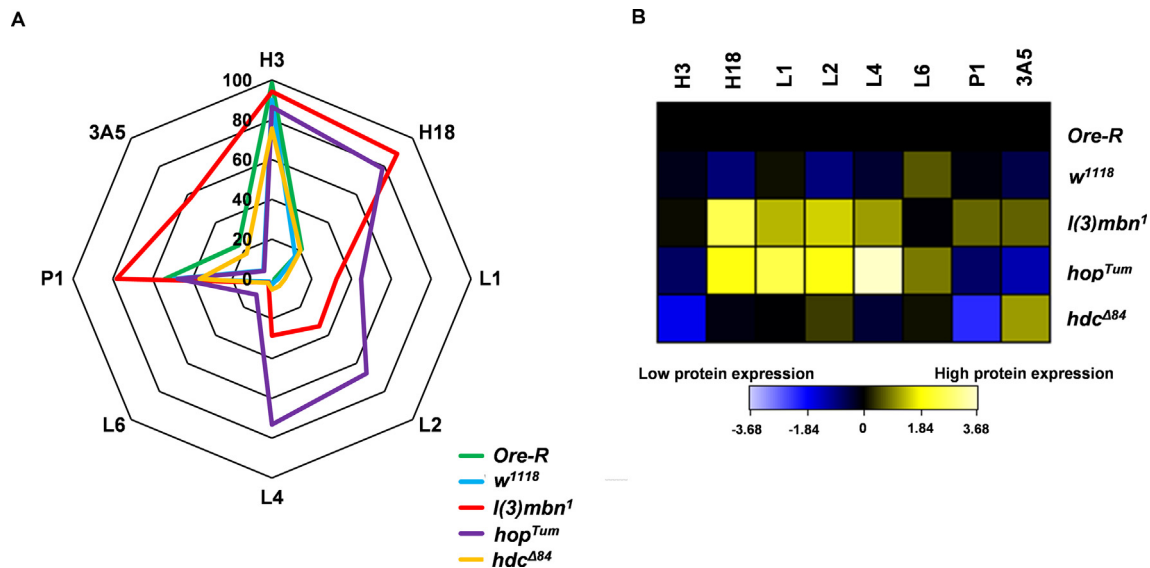
We built the metal tag-labeled panel of discriminative antibodies recognizing *Drosophila melanogaster* hemocytes and hemocyte subsets for mass cytometry in this study. We conjugated

Table 1 List of the antibodies used for mass cytometry

Antibody	Clone	Isotype	Metal tag	Refs.
Anti-H2 (Hemese)	1.2	Mouse IgG2a	147 Sm	[12,14]
Anti-H3	4A12	Mouse IgG1	155 Gd	[14]
Anti-H18 (Tetraspannin42Ed)	H18	Mouse IgG1	164 Dy	This study
Anti-L1 (Atilla)	H10	Mouse IgG1	149 Sm	[14,15,23]
Anti-L2	31A4	Mouse IgG2a	158 Gd	[14,23]
Anti-L4 (Integrin beta-PS)	1F12	Mouse IgG1	159 Tb	[14,23]
Anti-L6 (IgM)	H3	Mouse IgM	–	[14,23]
Anti-IgM	RMM-1	Rat IgG2a	172 Yb	[42]
Anti-P1 (NimC1)	N47	Mouse IgG1	154 Sm	[13,14,21]
Anti-3A5	3A5	Mouse IgG2b	169 Tm	This study
Anti-GFP	–	Rabbit polyclonal IgG	175 Lu	[43]
Anti-CD45	HI30	Mouse IgG1	89 Y	[44]

antibodies against six cell surface antigens (H2, H3, H18, L1, L4, and P1) and two intracellular antigens (3A5 and L2), as well as one anti-IgM for cell surface antigen L6. The list of antibodies can be found in **Table 1**. The anti-3A5 and anti-H18 antibodies first reported herein were characterized and validated by indirect immunofluorescence and Western blotting analyses (Figures S1 and S2). As shown in Figure S1, 3A5 is expressed in plasmatocytes and lamellocytes in *l(3)mbn¹* larvae, but not in lamellocytes of *L. boulandi* G486 immune-induced larvae (Figure S1). In contrast, H18 as a pan-hemocyte marker is expressed in all circulating hemocytes of samples tested (Figure S2). To optimize antibody efficacies, we compared the fluorescence-activated cell sorting (FACS) (Figure S3A) and mass cytometry histograms (Figure S3B) for the antibodies to various antigens. Both analyses showed similar reactivity patterns. Single living cells positive for the pan-hemocyte marker H2 were gated for mass cytometry analysis (Figure S4) and all metal tag-labeled antibodies were titrated for mass cytometry (Figure S5).

Next, we compared the expansion of hemocyte populations in the two mutant strains in relation to the two reference strains *Ore-R* and *w¹¹¹⁸*. The proportion of hemocytes expressing the investigated markers is comparable between *Ore-R* and *w¹¹¹⁸*. However, we detected the emergence of hemocytes expressing L1, L2, and L4 markers in *l(3)mbn¹* and *hop^{Tum}* mutant larvae, reflecting an extensive differentiation of lamellocytes, a phenotype characteristic to the blood cell malignancy. A slight elevation in the proportion of L6-expressing hemocytes was also detected in *hop^{Tum}* larvae (**Figure 1A**). This moderate change may be explained by the fact that L6 is only expressed in a subset of lamellocytes in tumorous larvae [14]. All lamellocyte markers showed a higher expression level in the tumorous *hop^{Tum}* mutant compared to the control stain *Ore-R* (**Figure 1B**, **Figure S7**). In the *hdc^{Δ84}* mutant larvae, we detected a moderate elevation in the expression level of L2, and a decrease in the expression level of P1 (**Figure 1B**). However, the proportion of hemocytes expressing lamellocyte markers in the *hdc^{Δ84}* strain did not increase

**Figure 1** SCMC revealed the expansion of hemocytes in *hop^{Tum}* and *l(3)mbn¹*

A. The percentages of hemocytes expressing H3, H18, L1, L2, L4, L6, P1, and 3A5 were plotted on radar plots for *Drosophila* mutants on the *Ore-R* or *w¹¹¹⁸* background. **B.** Comparative heatmap of mass cytometry data (arcsinh-transformed median intensity values) regarding marker density at single-cell resolution showed increased expression of H18, L1, L2, and L4 markers in the *hop^{Tum}* and *l(3)mbn¹* mutants in relation to the control, the wild-type *Ore-R*. The analysis was performed within the H2-positive live singlets. SCMC, single-cell mass cytometry.

significantly compared to the controls (Figure 1A). This is in line with the finding that in the *hdc^{Δ84}* mutant larvae, lamellocytes differentiate in low numbers, while the number of plasmatocytes is reduced [30]. A reduction in the proportion of plasmatocytes was also evident in the *hdc^{Δ84}* larvae (Figure 1A).

Multidimensional analysis by the t-distributed stochastic neighbor embedding (tSNE) algorithm and the visualization of t-distributed stochastic neighbor embedding (viSNE) was carried out within the H2-positive live singlets based on the expression of H3, H18, L1, L2, L4, L6, P1, and 3A5 markers in order to map high-parametric single-cell data on biaxial plots [34]. The viSNE patterns of hemocyte marker expression (Figure 2) correlated to the data shown in Figure 1. The viSNE bioinformatic analysis revealed the characteristic protein expression patterns of hemocyte subsets at single-cell resolution from the studied genetic variants. We observed a dramatic difference in the viSNE patterns between hemocytes isolated from the tumorous *l(3)mbn¹* and *hop^{Tum}* larvae and those isolated from either *Ore-R* or *w¹¹¹⁸* control larvae (Figure 2). *Ore-R* and *w¹¹¹⁸* hemocytes were not discriminated on the viSNE plots, showing their minimal genetic distance, but tumorous *l(3)mbn¹* and *hop^{Tum}* larvae delineated viSNE maps with the expansion of lamellocytes (Figure 2). In the *hdc^{Δ84}* larvae, we detected a subset of hemocytes that express the 3A5 marker at a high level. This subset was detected neither

in control nor in the tumorous larvae, and may represent a cell type that differentiates as a precursor for lamellocytes as a consequence of the defect in the maintenance of the hematopoietic niche [30].

The Uniform Manifold Approximation and Projection (UMAP) analysis was performed on the five studied genetic variants of *Drosophila melanogaster* by using the hemocyte subset-specific, discriminating markers: L1, L2, L4, and L6 for lamellocytes, and P1 for plasmatocytes. The UMAP analysis resulted in the same conclusion as tSNE, namely that lamellocyte expansion occurs in tumorous strains *l(3)mbn¹* and *hop^{Tum}* (Figure S8). Both the viSNE and UMAP analyses demonstrate the transitional phenotypes of certain lamellocytes and plasmatocytes by the co-expression of L2/P1 and L2/L4/P1 in *l(3)mbn¹* and *hop^{Tum}*, respectively (Figure 2, Figure S8). Merging viSNE graphs outlined characteristic maps of each strain based on high-parametric mass cytometry data (Figure 3A–C). The *Ore-R* and *w¹¹¹⁸* controls showed overlapping patterns on the viSNE diagram (Figure 3A–C), with a somewhat lower expression of all markers tested except for L6 in *w¹¹¹⁸* (Figure 1B), which may be due to uncontrollable genetic background variations. The dots representing the hemocytes from *hdc^{Δ84}*, a mutant of the *hdc* regulator of hematopoietic stem cell maintenance [30], were detected as a zone in between the control and the tumorous patterns (Figure 3C). The most likely explanation to this phenomenon

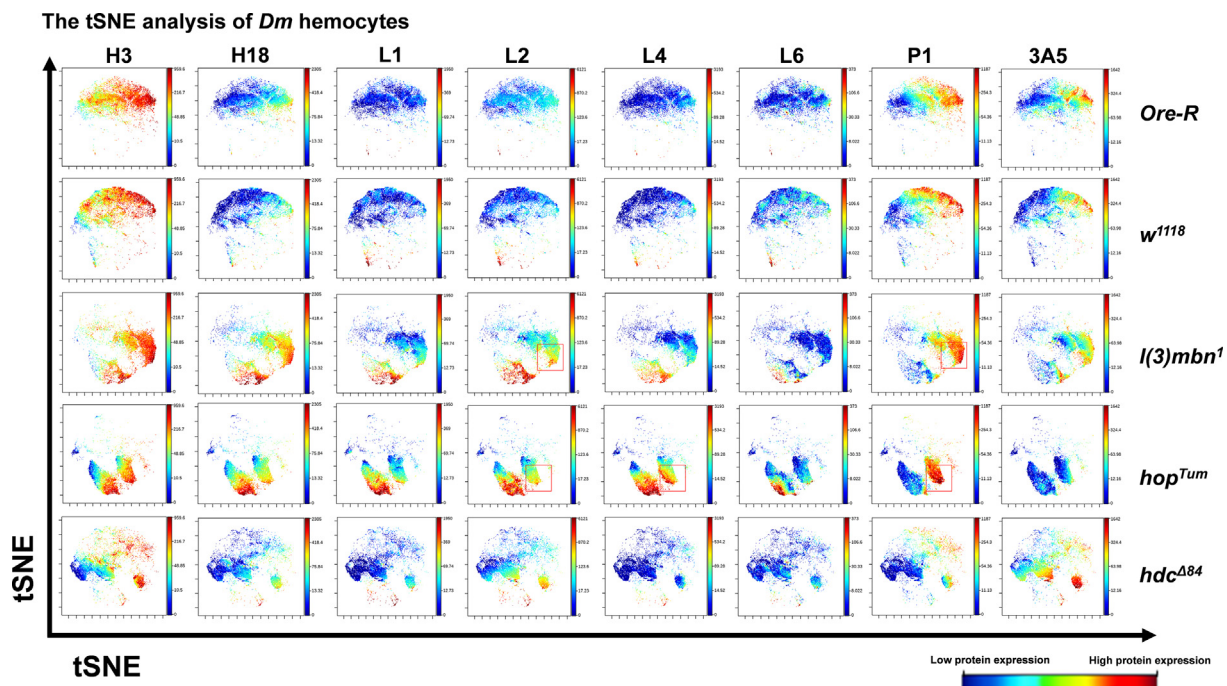


Figure 2 Multidimensional comparative analysis by the tSNE algorithm

The tSNE algorithm dissects the cell relatedness of five different *Drosophila* strains, namely *Ore-R*, *w¹¹¹⁸*, *l(3)mbn¹*, *hop^{Tum}*, and *hdc^{Δ84}*. The wild-type *Ore-R* and white mutant *w¹¹¹⁸* (genetic backgrounds) displayed overlapping expression patterns of all markers tested, while both tumorous strains *l(3)mbn¹* and *hop^{Tum}* showed H18, L1, L2, and L4 expansion. The tSNE analysis of H3, H18, L1, L2, L4, L6, P1, and 3A5 markers was carried out within the population of pan-hemocyte H2-positive live singlets and visualized as viSNE plots. Subpopulations of cells with common marker expression patterns are grouped close in the multidimensional space, while cells with different marker expression are plotted separately. Coloration is proportional to the expression intensity of a given marker: the hotter the plot, the higher the level of expression (red plots). Red boxes mark transitional phenotypes expressing both lamellocyte (L2 or L4) and plasmatocyte (P1) markers. tSNE, t-distributed stochastic neighbor embedding; viSNE, visualization of t-distributed stochastic neighbor embedding; *Dm*, *Drosophila melanogaster*.

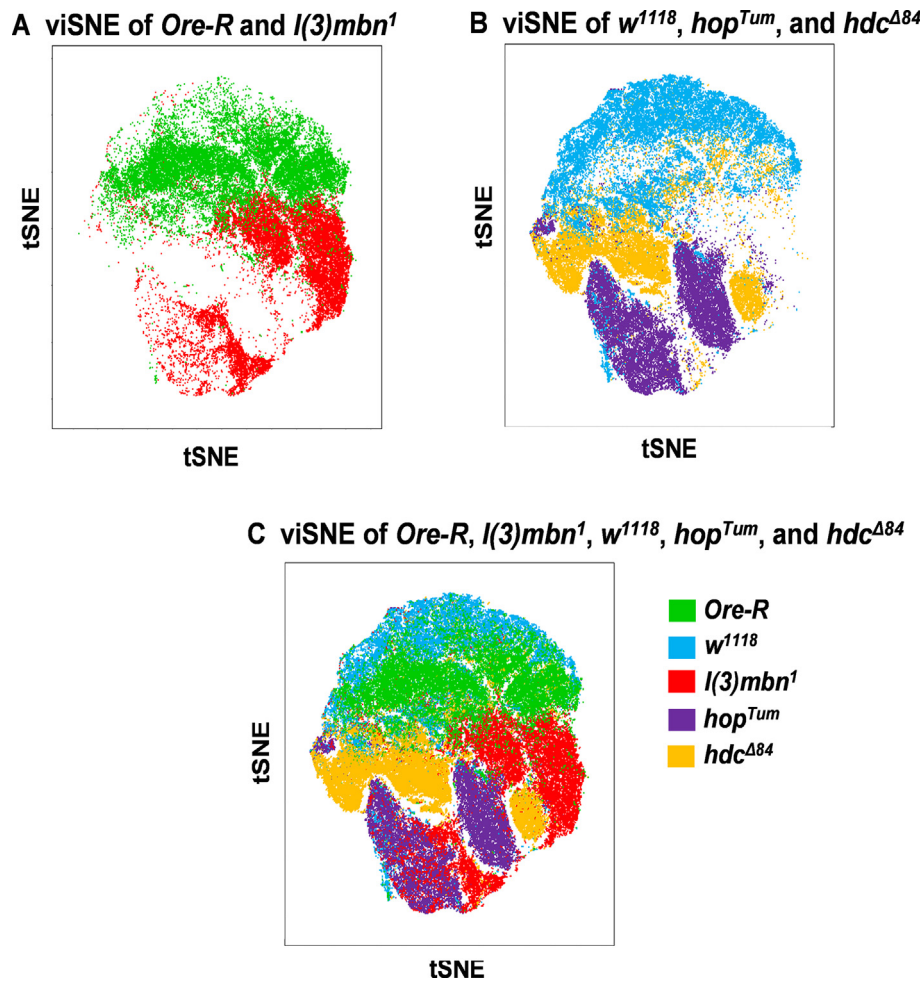


Figure 3 Merging viSNE graphs outlined characteristic maps of each strain

The tSNE analysis was based on expression of H3, H18, L1, L2, L4, L6, P1, and 3A5 markers within the pan-hemocyte H2-positive live singlets. **A.** The viSNE comparison of *l(3)mbn*¹ and its wild-type counterpart *Ore-R*. **B.** The viSNE comparison of *w*¹¹¹⁸, *hop*^{Tum}, and *hdc*^{Δ84}. **C.** The viSNE islands of hemocytes from the *Ore-R* and *w*¹¹¹⁸ control strains localize separately from the tumorous *l(3)mbn*¹ and *hop*^{Tum} hemocytes, while the hemocytes from *hdc*^{Δ84} represent a transition phenotype.

is that *hdc*^{Δ84} homozygous larvae produce lamellocytes, but in a much lower proportion than tumorous larvae, *l(3)mbn*¹ and *hop*^{Tum} [30]. Tumorous hemocytes from *l(3)mbn*¹ and *hop*^{Tum} were closely mapped and partially overlapping, giving a population clearly separated from the cloud of the controls due to the lamellocyte-expansive malignant phenotype (Figure 3C).

SCMC reveals the transitional phenotypes of hemocytes upon immune induction

In order to monitor the changes in the composition of hemocyte subsets following immune induction, we used the *lz* > GFP larvae and complemented the experiment with anti-GFP labeling, which enables the detection of crystal cells in that particular strain [32,33]. The tSNE analysis of the H3, H18, L1, L2, L4, L6, P1, 3A5 markers and the GFP reporter was carried out within the population of pan-hemocyte H2-positive live singlets (Figure 4A). We observed a new subset of hemocytes appearing 72 h after the infestation of the *lz* > GFP larvae with the *L. boulandi* parasitoid wasp (Fig-

ure 4A, Figure S9). This subset of cells accounts for the lamellocytes that differentiate as a result of the immune induction since these cells fall into the high expression part of the viSNE for the L1, L2, L4, and L6 lamellocyte markers (Figure 4A, Figure S9). This finding is in correlation with an increase in the percentage of hemocytes expressing L1 (35.10% vs. 1.81%), L2 (32.09% vs. 1.64%), L4 (34.36% vs. 1.39%), and L6 (13.82% vs. 0.94%) markers (Figure 4B), and the elevated expression levels of lamellocyte markers detected in immune induced larvae compared to the naive control (Figure 4C). Interestingly, a new subset of crystal cells (GFP-positive cells) appeared in immune-induced larvae (*lz* > GFP *i.i.*) compared to the naive control (*lz* > GFP) (Figure 4A). The viSNE pattern of the 3A5 marker also changed significantly after the immune induction (Figure 4A), which may be due to the newly differentiating hemocytes, similarly to that observed in the *hdc*^{Δ84} larvae.

Taken together, we report herein the first panel of metal-conjugated anti-*Drosophila* antibodies to present the applicability of mass cytometry for that canonical model organism of genetics. Recent studies have identified novel subpopula-

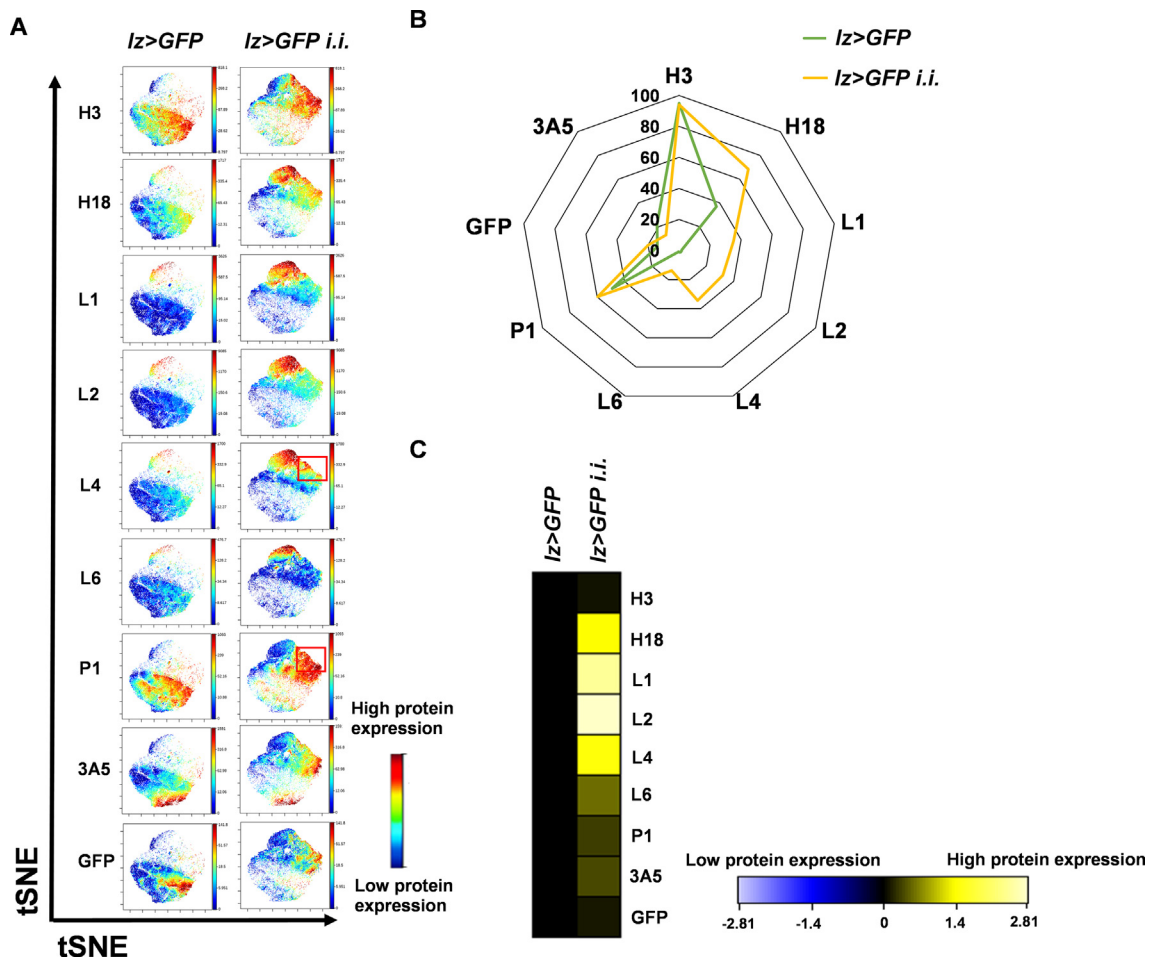


Figure 4 Immune activation by infestation with the *Leptopilina boulandi* parasitoid wasp of the *lz > GFP* strain

A. viSNE analysis of naive (*lz > GFP*) and immune-induced (*lz > GFP i.i.*) *Drosophila* larvae. The tSNE analysis of the H3, H18, L1, L2, L4, L6, P1, and 3A5 markers and the GFP reporter was carried out within the population of pan-hemocyte H2-positive live singlets. Red boxes mark a subpopulation, the transitional phenotype of hemocytes expressing both lamellocyte (L4⁺) and plasmatocyte (P1⁺) markers upon immune induction. **B.** The percentages of hemocytes positive for H3, H18, L1, L2, L4, L6, P1, GFP (crystal cells), and 3A5. **C.** The heatmap of the median values (arcsinh-transformed) shows the expression changes of the hemocyte marker expression upon immune induction. The analysis was performed within the pan-hemocyte marker H2-positive live singlets. GFP, crystal cells marked by the expression of GFP in this particular system.

tions of *Drosophila* hemocytes based on single-cell RNA data [35–38]. These findings have largely contributed to the definition of hemocyte clusters and to the characterization of intermediate cells in the transition from plasmatocyte to lamellocyte. In these experiments, clusters were defined by the gene expression patterns of individual hemocytes. The application of “cytometry by time-of-flight” (CyTOF) can complement these comprehensive transcriptomic studies and verify the existence of transitional phenotypes at the protein level. The comparative analysis of *Ore-R* and *w¹¹¹⁸* with *l(3)mbn¹*, *hop^{Tum}*, and *hdc^{Δ84}* revealed transitional phenotypes at the protein level and the differences among reference stains: *Ore-R* and *w¹¹¹⁸*. Both the viSNE and UMAP analyses demonstrated the transitional phenotypes of certain subpopulations of lamellocytes and plasmatocytes by the co-expression of L2/P1 and L2/L4/P1 in *l(3)mbn¹* and *hop^{Tum}*, respectively. This has been verified by a functional assay of immune induction (Figure 4). Our study demonstrates transitional phenotypes (Figure 2, Figure 4A, Figure S8) from single-cell

data at the protein level, which places the innate immunity of *Drosophila* in a new biological insight. Additionally, we report herein two novel hemocyte markers, 3A5 with intracellular localization and H18 located on the cell surface. The simultaneous detection of several antigens provided by CyTOF could not be achieved earlier by traditional microscopy.

The main advantage of CyTOF is the multidimensionality coupled with complex computational tools; therefore we propose the extension of the basic panel used in our study with antibodies recognizing signaling molecules (e.g., MAP kinases), enzymes (to follow metabolic pathways), and cellular structural proteins (e.g., cytoskeletal and cargo proteins) up to 42 markers in one single tube. Another advantage of the presented method is that CyTOF enables investigations at the protein level (data of transcriptomics should be verified at the protein level) with single-cell resolution. However, we may consider the main limitation of the CyTOF, i.e., the availability of antibodies against the protein of interest, which is also a limitation for other antibody-based detection

approaches. Moreover, anti-tag antibodies are available when the protein of interest is labeled with a fusion tag, or the cell of interest is labeled with the expression of a marker protein (we report herein the use of anti-GFP). Other limitations are the availability of the CyTOF technology (it is increasing and most of the research centers are supposed to own the technology, as there were 94 instruments already installed in Europe in 2020 January), and the relatively high cost of the CyTOF technology (although the cost should be taken into account by the number of investigated markers at the protein level and the number of single cells).

We believe that our method serves as a rapid and cost-effective tool to monitor the alteration of hemocyte composition influenced by various agents or mutations. In those cases, it is less expensive and easier to perform than single-cell transcriptome analysis. Additionally, the CyTOF can complement transcriptomic studies verifying up to 42 simultaneous markers at the protein level with single-cell resolution.

Conclusion

The SCMC combines the features of traditional cytometry with mass spectrometry and enables the detection of several parameters at single-cell resolution, thus permitting a complex analysis of biological regulatory mechanisms. We optimized this platform to analyze the cellular elements, the hemocytes of the *Drosophila* innate immune system. The SCMC analysis with 9 antibodies to all hemocytes and hemocyte subsets showed good accordance of fluorescence flow cytometry results in terms of positivity on hemocytes of the tumor suppressor mutant *l(3)mbn¹*. Further, we investigated the antigen expression profile of single cells and hemocyte populations in control strains (*Ore-R* and *w¹¹¹⁸*) and tumorous strains (*l(3)mbn¹* and *hop^{Tum}*), as well as in a stem cell maintenance defective mutant (*hdc^{A84}*). The immunophenotype of immune activation upon infestation with a parasitoid wasp and the differentiation of lamellocytes were detected by 10 antibodies in the *lz > GFP* larvae.

Multidimensional analysis (viSNE) enabled the discrimination of the major hemocytes: lamellocytes, plasmatocytes, and crystal cells, and delineated the unique single-cell immunophenotype of the mutant strains under investigation. SCMC identified subpopulations of L2⁺/P1⁺ and L2⁺/L4⁺/P1⁺ transitional phenotype cells in the tumorous strains *l(3)mbn¹* and *hop^{Tum}*, respectively, and a subpopulation of L4⁺/P1⁺ cells upon immune induction. We demonstrated that mass cytometry, a recent single-cell technology coupled with multidimensional bioinformatic analysis at the protein level, represents a powerful tool to deeply analyze *Drosophila*, a key multicellular model organism of genetic studies with a wide inventory of available mutants.

Materials and methods

Drosophila stocks

The following *Drosophila* lines were used in the current study: *w¹¹¹⁸* (BSC#9505, Bloomington *Drosophila* Stock Center,

Bloomington, IN), *Ore-R* (wild type), *w*; *hdc^{A84}/TM3, Kr > GFP* [30], *lz-Gal4, UAS-GFP*; +; + (a gift from Bruno Lemaitre, Lausanne, Switzerland) [32], *l(3)mbn¹/TM6 Tb* [28], and a homozygous *hop^{Tum}* (BSC#8492) line generated by Dr. Gábor Csordás (BRC, Szeged, Hungary). The flies were grown on a standard cornmeal-yeast substrate at 25 °C.

Production of 3A5 and H18 antibodies

Monoclonal antibodies against *Drosophila* hemocytes were raised as described previously [14]. Briefly, BALB/c mice were immunized by intraperitoneal injection of 1×10^6 hemocytes from late third instar larvae of the *l(3)mbn¹* mutant in *Drosophila* Ringer's solution (Sigma-Aldrich, St. Louis, MI). Booster injections were given 4, 8, and 13 weeks later. Three days after the last immunization, spleen cells were collected and fused with SP2/O myeloma cells by using polyethylene glycol (PEG1450; catalog No. P5402, Sigma-Aldrich). Hybridomas were selected in hypoxanthine-aminopterin-thymidine (HAT) supplement medium (Catalog No. 21060017, ThermoFischer Scientific, Waltham, MA) and maintained as described by Kohler and Milstein [14,39]. Hybridoma culture supernatants were screened by indirect immunofluorescence on live or acetone-fixed permeabilized hemocytes. The selected hybridomas were subcloned three times by limiting dilution.

Isolation of hemocytes

Hemocytes were isolated from late third stage larvae by dissecting the larvae in *Drosophila* Schneider's solution (Catalog No. 21720001, ThermoFisher Scientific) supplemented with 5% fetal bovine serum (FBS; Catalog No. F7524-500ML, Sigma-Aldrich) plus 0.003% 1-phenyl-2-thiourea (Catalog No. P7629, Sigma-Aldrich).

Immune induction

lz > GFP flies laid eggs for three days in bottles containing standard *Drosophila* medium. After 72 h, larvae were infected with *L. boulandi* wasps for 6 h. Larvae with visible melanotic nodules were selected 72 h after infestation for isolation of hemocytes. Age and size-matched larvae were used as control.

Immunofluorescent staining

Immunofluorescent staining was performed as described previously [23]. Briefly, hemocytes were attached to multispot slides (Catalog No. SM-011, Hendley-Essex, Loughton, UK) at 21 °C for 45 min. Slides were fixed with acetone for 6 min, rehydrated, blocked for 20 min in phosphate-buffered saline (PBS; catalog No. P4417, Sigma-Aldrich) supplemented with 0.1% bovine serum albumin (BSA; catalog No. A2058, Sigma-Aldrich), incubated with the indicated antibodies for 1 h at 21 °C, washed three times with PBS, and incubated with CF-568-conjugated anti-mouse IgG (H + L), F(ab')₂ fragment (1:1000; catalog No. SAB4600082, Sigma-Aldrich) for 45 min. Nuclei were labeled with DAPI (Catalog No. D9542, Sigma-Aldrich). The microscopic analysis was carried out using a Zeiss AxioScope 2MOT epifluorescent microscope

and Axiovision 2.4 software (Zeiss, Oberkochen, Germany).

Western blotting

Western blotting was performed in order to test the specificity of the anti-3A5 and anti-H18 antibodies, as described previously [12]. Briefly, proteins were separated by SDS-PAGE. Following the electrophoresis, the proteins were blotted onto a nitrocellulose membrane (Hybond-C; catalog No. 10564755, Amersham Pharmacia, Buckinghamshire, UK) in the transfer buffer [25 mM Tris pH 8.3, 192 mM glycine, 20% (V/V) methanol]. The nonspecific binding was blocked with PBS supplemented with 0.1% Tween 20 (PBST; catalog No. P1379, Sigma-Aldrich) and 5% non-fat dry milk at 21 °C for 1 h. The blotted proteins were reacted to the indicated antibody (anti-3A5 in Figure S1, and anti-H18 in Figure S2) with rotation at 21 °C for 3 h. Washing was performed with PBST three times for 10 min, followed by incubation with HRPO-conjugated anti-mouse antibody (Catalog No. 62-6520, ThermoFisher Scientific). After three washes with PBST for 10 min, the proteins were detected by the ECL-Plus system (Catalog No. 32132, ThermoFisher Scientific) following the manufacturer's recommendations.

Flow cytometry

Flow cytometry was executed as published previously [12]. Briefly, 20 µl of 1×10^7 /ml hemocyte suspension was plated into each well of a 96-well U-bottom microtiter plate (Catalog No. 3635, Corning Life Sciences, Tewksbury, MA) containing insect Schneider's medium [supplemented with 10% fetal calf serum (Gibco, Thermo Fisher Scientific). Samples for intracellular staining were treated with 2% paraformaldehyde (Catalog No. 158127, Sigma-Aldrich). Hybridoma supernatants (50 µl) were measured to each well and reacted at 4 °C for 45 min. The negative control monoclonal antibody was a mouse IgG1 (clone T2/48, anti-human CD45) [40]. After the incubation, cells were washed three times with ice-cold Schneider's medium. The secondary antibody, Alexa Fluor 488-labeled anti-mouse IgG (Catalog No. AP124JA4, Sigma-Aldrich) was added (1:1000). After 45 min incubation at 4 °C, the cells were washed three times with ice-cold Schneider's medium and acquired on FACSCalibur (Beckton Dickinson, Franklin Lakes, NJ).

Mass cytometry

Mass cytometry was performed as we published earlier with some modifications [10,41]. The affinity-purified monoclonal antibodies were provided by István Andó's group (BRC, Szeged, Hungary) or purchased: anti-IgM (Catalog No. 406527, Biolegend, San Diego, CA, [42]), anti-GFP (Catalog No. A11122, ThermoFisher Scientific [43]), and anti-CD45 (Catalog No. 3089003B, Fluidigm, South San Francisco, CA [44]), and then conjugated in house using Maxpar Antibody Labeling Kit (Fluidigm) according to the instructions of the manufacturer. Optimal antibody concentrations were titrated prior to use (Figure S5). The following antibody concentrations were used: anti-H2: 5 µg/ml, anti-H3: 5 µg/ml, anti-H18: 5 µg/ml, anti-L1: 1 µg/ml, anti-L2: 7.5 µg/ml, anti-L4: 7.5 µg/ml, anti-L6: 10 µg/ml, anti-IgM:

10 µg/ml, anti-P1: 7.5 µg/ml, anti-3A5: 5 µg/ml, and anti-GFP: 10 µg/ml. The L6 (IgM isotype) marker was measured indirectly via metal tag-labeled anti-IgM antibody. The negative control monoclonal antibody was a mouse IgG1 (clone HI30, anti-human 89 Y-labeled CD45) in 1:100 dilution. The isotypes of anti-*Drosophila* antibodies were determined by the IsoStrip™ Antibody Isotyping Kit (Catalog No. 11493027001, Roche, Basel, Switzerland) according to the instructions of the manufacturer.

Single-cell suspensions were centrifugated at 1100 g at 6 °C for 4 min and incubated with viability marker (5 µM cisplatin, 195 Pt; catalog No. 201064, Fluidigm) on ice in 40 µl PBS for 3 min. Cells were washed twice with 200 µl Maxpar Cell Staining Buffer (MCSB; catalog No. 201068, Fluidigm) and centrifugated at 1100 g at 6 °C for 4 min. Cells were resuspended in 50 µl MCSB, and then 50 µl surface antibody cocktail (2×) was added and incubated on ice for 30 min. Cells were washed with 200 µl MCSB, stained with anti-IgM antibody (volumes were the same as in the surface staining), and incubated on ice for 30 min. Cells were washed with 200 µl MCSB, suspended in 100 µl 1× Maxpar Fix I buffer (Catalog No. 201065, Fluidigm), and incubated on ice for 20 min. Cells were washed twice with 200 µl Perm-S buffer (Catalog No. 201066, Fluidigm), stained with the intracellular antibody cocktail (anti-L2, anti-3A5, and anti-GFP in *Lz > GFP* samples), and left on ice for 30 min. Cells were washed once with MCSB, fixed with 200 µl of 1.6% formaldehyde solution [freshly diluted from 16% Pierce formaldehyde (Catalog No. 28906, ThermoFisher Scientific) in PBS], incubated on ice for 10 min, and then centrifugated at 1300 g at 6 °C for 4 min. After fixation, cells were resuspended in 300 µl Maxpar Fix and Perm buffer (Catalog No. 201067, Fluidigm) containing 125 nM Cell-ID DNA intercalator (191/193 Iridium; catalog No. 201192A, Fluidigm) and incubated at 4 °C overnight. Before the acquisition, samples were washed in MCSB twice and in PBS (without Mg^{2+} and Ca^{2+} ; catalog No. 10010015, ThermoFisher Scientific) once by centrifugation at 1300 g at 6 °C for 4 min. Cells were counted using the Bürker chamber. For the measurement on Helios, the concentration of cells was set to 0.5×10^6 /ml in cell acquisition solution (CAS; catalog No. 201240, Fluidigm) supplemented with 10% EQ Calibration Beads (Catalog No. 201078, Fluidigm). Cells were filtered with Celltrics (30 µm; catalog No. 04-0042-2316, Sysmex Partec, Görlitz, Germany) prior to acquisition. Samples were run on CyTOF Helios (Fluidigm). Bead-based normalization of CyTOF data was performed. After randomization, normalization, and FCS file generation, the files were further analyzed in Cytobank (Beckman Coulter, Brea, CA). Analysis of the cells was carried out on live singlets within the pan-hemocyte marker H2-positive population. The viSNE analysis was carried out on 3×10^4 cisplatin-negative (live) singlets with the following settings: iterations = 1000, perplexity = 30, theta = 0.5.

CRedit author statement

József Á. Balog: Data curation, Formal analysis, Investigation, Methodology, Software, Validation, Visualization. **Viktor Honti:** Conceptualization, Data curation, Formal analysis, Investigation, Methodology, Writing - original draft, Writing - review & editing. **Éva Kurucz:** Data curation, Formal analysis, Investigation, Methodology, Writing - review & editing. **Beáta Kari:** Investigation. **László G. Puskás:** Conceptualiza-

tion, Funding acquisition, Project administration, Resources, Supervision, Writing - review & editing. **István Andó:** Conceptualization, Formal analysis, Funding acquisition, Project administration, Resources, Supervision, Writing - original draft, Writing - review & editing. **Gábor J. Szebeni:** Conceptualization, Formal analysis, Project administration, Supervision, Writing - original draft, Writing - review & editing. All authors read and approved the final manuscript.

Competing interests

The authors have declared no competing interests.

Acknowledgments

This work was supported by the grants from the National Research, Development and Innovation Office, Hungary (Grant Nos. GINOP-2.3.2-15-2016-00001, GINOP-2.3.2-15-2016-00030 to LGP, GINOP-2.3.2-15-2016-00035 to ÉK, NKFI NN118207 and NKFI K120142 to IA, NKFI 120140 to ÉK, and OTKA K-131484 to VH). Gábor J. Szebeni was supported by the New National Excellence Program of the Ministry for Innovation and Technology, Hungary (Grant No. UNKP-19-4-SZTE-36) and by the János Bolyai Research Scholarship of the Hungarian Academy of Sciences (Grant No. BO/00139/17/8). We are grateful to Mrs. Olga Kovalcsik for the technical help.

Supplementary material

Supplementary data to this article can be found online at <https://doi.org/10.1016/j.gpb.2020.06.022>.

ORCID

0000-0001-8208-9157 (József Á. Balog)
 0000-0001-7418-3653 (Viktor Honti)
 0000-0002-9386-2798 (Éva Kurucz)
 0000-0002-4377-6824 (Beáta Kari)
 0000-0003-0271-3517 (László G. Puskás)
 0000-0002-4648-9396 (István Andó)
 0000-0002-6998-5632 (Gábor J. Szebeni)

References

- [1] Kim-Jo C, Gatti JL, Poirie M. *Drosophila* cellular immunity against parasitoid wasps: a complex and time-dependent process. *Front Physiol* 2019;10:603.
- [2] Troha K, Buchon N. Methods for the study of innate immunity in *Drosophila melanogaster*. *Wiley Interdiscip Rev Dev Biol* 2019;8:e344.
- [3] Imler JL, Bulet P. Antimicrobial peptides in *Drosophila*: structures, activities and gene regulation. *Chem Immunol Allergy* 2005;86:1–21.
- [4] Williams MJ. *Drosophila* hemopoiesis and cellular immunity. *J Immunol* 2007;178:4711–6.
- [5] Loch G, Zinke I, Mori T, Carrera P, Schroer J, Takeyama H, et al. Antimicrobial peptides extend lifespan in *Drosophila*. *PLoS One* 2017;12:e0176689.
- [6] Kenmoku H, Hori A, Kuraishi T, Kurata S. A novel mode of induction of the humoral innate immune response in *Drosophila* larvae. *Dis Model Mech* 2017;10:271–81.
- [7] Evans CJ, Liu T, Banerjee U. *Drosophila* hematopoiesis: markers and methods for molecular genetic analysis. *Methods* 2014;68:242–51.
- [8] Goto A, Kadowaki T, Kitagawa Y. *Drosophila* hemolectin gene is expressed in embryonic and larval hemocytes and its knock down causes bleeding defects. *Dev Biol* 2003;264:582–91.
- [9] Tokusumi T, Shoue DA, Tokusumi Y, Stoller JR, Schulz RA. New hemocyte-specific enhancer-reporter transgenes for the analysis of hematopoiesis in *Drosophila*. *Genesis* 2009;47:771–4.
- [10] Alfoldi R, Balog JA, Farago N, Halmai M, Kotogany E, Neuperger P, et al. Single cell mass cytometry of non-small cell lung cancer cells reveals complexity of *in vivo* and three-dimensional models over the Petri-dish. *Cells* 2019;8:1093.
- [11] Bandyopadhyay S, Fowles JS, Yu L, Fisher DAC, Oh ST. Identification of functionally primitive and immunophenotypically distinct subpopulations in secondary acute myeloid leukemia by mass cytometry. *Cytometry B Clin Cytom* 2019;96:46–56.
- [12] Kurucz E, Zettervall CJ, Sinka R, Vilmos P, Pivarsci A, Ekengren S, et al. Hemese, a hemocyte-specific transmembrane protein, affects the cellular immune response in *Drosophila*. *Proc Natl Acad Sci U S A* 2003;100:2622–7.
- [13] Kurucz E, Markus R, Zsamboki J, Folkl-Medzihradsky K, Darula Z, Vilmos P, et al. Nimrod, a putative phagocytosis receptor with EGF repeats in *Drosophila* plasmatocytes. *Curr Biol* 2007;17:649–54.
- [14] Kurucz E, Vaczi B, Markus R, Laurinyecz B, Vilmos P, Zsamboki J, et al. Definition of *Drosophila* hemocyte subsets by cell-type specific antigens. *Acta Biol Hung* 2007;58:95–111.
- [15] Honti V, Kurucz E, Csordas G, Laurinyecz B, Markus R, Ando I. *In vivo* detection of lamellocytes in *Drosophila melanogaster*. *Immunol Lett* 2009;126:83–4.
- [16] Anderl I, Vesala L, Ihalainen TO, Vanha-Aho LM, Ando I, Ramet M, et al. Transdifferentiation and proliferation in two distinct hemocyte lineages in *Drosophila melanogaster* larvae after wasp infection. *PLoS Pathog* 2016;12:e1005746.
- [17] Honti V, Csordas G, Kurucz E, Markus R, Ando I. The cell-mediated immunity of *Drosophila melanogaster*: hemocyte lineages, immune compartments, microanatomy and regulation. *Dev Comp Immunol* 2014;42:47–56.
- [18] Nappi AJ, Vass E, Frey F, Carton Y. Superoxide anion generation in *Drosophila* during melanotic encapsulation of parasites. *Eur J Cell Biol* 1995;68:450–6.
- [19] Russo J, Dupas S, Frey F, Carton Y, Brehelin M. Insect immunity: early events in the encapsulation process of parasitoid (*Leptopilina boulardi*) eggs in resistant and susceptible strains of *Drosophila*. *Parasitology* 1996;112:135–42.
- [20] Lanot R, Zachary D, Holder F, Meister M. Postembryonic hematopoiesis in *Drosophila*. *Dev Biol* 2001;230:243–57.
- [21] Melcarne C, Ramond E, Dudzic J, Bretscher AJ, Kurucz E, Ando I, et al. Two Nimrod receptors, NimC1 and Eater, synergistically contribute to bacterial phagocytosis in *Drosophila melanogaster*. *FEBS J* 2019;286:2670–91.
- [22] Avet-Rochex A, Boyer K, Polesello C, Gobert V, Osman D, Roch F, et al. An *in vivo* RNA interference screen identifies gene networks controlling *Drosophila melanogaster* blood cell homeostasis. *BMC Dev Biol* 2010;10:65.
- [23] Honti V, Csordas G, Markus R, Kurucz E, Jankovics F, Ando I. Cell lineage tracing reveals the plasticity of the hemocyte lineages and of the hematopoietic compartments in *Drosophila melanogaster*. *Mol Immunol* 2010;47:1997–2004.

- [24] Stofanko M, Kwon SY, Badenhorst P. Lineage tracing of lamellocytes demonstrates *Drosophila* macrophage plasticity. *PLoS One* 2010;5:e14051.
- [25] Kroeger Jr PT, Tokusumi T, Schulz RA. Transcriptional regulation of eater gene expression in *Drosophila* blood cells. *Genesis* 2012;50:41–9.
- [26] Mirzoyan Z, Sollazzo M, Allocca M, Valenza AM, Grifoni D, Bellosta P. *Drosophila melanogaster*: a model organism to study cancer. *Front Genet* 2019;10:51.
- [27] Harrison DA, Binari R, Nahreini TS, Gilman M, Perrimon N. Activation of a *Drosophila* Janus kinase (JAK) causes hematopoietic neoplasia and developmental defects. *EMBO J* 1995;14:2857–65.
- [28] Konrad L, Becker G, Schmidt A, Klockner T, Kaufer-Stillger G, Dreschers S, et al. Cloning, structure, cellular localization, and possible function of the tumor suppressor gene *lethal(3)malignant blood neoplasm-1* of *Drosophila melanogaster*. *Dev Biol* 1994;163:98–111.
- [29] Weaver TA, White RA. *Headcase*, an imaginal specific gene required for adult morphogenesis in *Drosophila melanogaster*. *Development* 1995;121:4149–60.
- [30] Varga GIB, Csordas G, Cinege G, Jankovics F, Sinka R, Kurucz E, et al. *Headcase* is a repressor of lamellocyte fate in *Drosophila melanogaster*. *Genes (Basel)* 2019;10:173.
- [31] Ferreira MJ, Perez C, Marchesano M, Ruiz S, Caputi A, Aguilera P, et al. *Drosophila melanogaster white* mutant *w¹¹¹⁸* undergo retinal degeneration. *Front Neurosci* 2017;11:732.
- [32] Binggeli O, Neyen C, Poidevin M, Lemaitre B. Prophenoloxidase activation is required for survival to microbial infections in *Drosophila*. *PLoS Pathog* 2014;10:e1004067.
- [33] Lebestky T, Chang T, Hartenstein V, Banerjee U. Specification of *Drosophila* hematopoietic lineage by conserved transcription factors. *Science* 2000;288:146–9.
- [34] Amir el AD, Davis KL, Tadmor MD, Simonds EF, Levine JH, Bendall SC, et al. viSNE enables visualization of high dimensional single-cell data and reveals phenotypic heterogeneity of leukemia. *Nat Biotechnol* 2013;31:545–52.
- [35] Cho B, Yoon SH, Lee D, Koranteng F, Tattikota SG, Cha N, et al. Single-cell transcriptome maps of myeloid blood cell lineages in *Drosophila*. *Nat Commun* 2020;11:4483.
- [36] Merkling SH, Lambrechts L. Taking insect immunity to the single-cell level. *Trends Immunol* 2020;41:190–9.
- [37] Cattenoz PB, Sakr R, Pavlidaki A, Delaporte C, Riba A, Molina N, et al. Temporal specificity and heterogeneity of *Drosophila* immune cells. *EMBO J* 2020;39:e104486.
- [38] Tattikota SG, Cho B, Liu Y, Hu Y, Barrera V, Steinbaugh MJ, et al. A single-cell survey of *Drosophila* blood. *Elife* 2020;9:e54818.
- [39] Kohler G, Milstein C. Derivation of specific antibody-producing tissue culture and tumor lines by cell fusion. *Eur J Immunol* 1976;6:511–9.
- [40] Oravecz T, Monostori E, Kurucz E, Takacs L, Ando I. Cd3-induced T-cell proliferation and interleukin-2 secretion is modulated by the CD45 antigen. *Scand J Immunol* 1991;34:531–7.
- [41] Balog JA, Hackler Jr L, Kovacs AK, Neuperger P, Alfoldi R, Nagy LI, et al. Single cell mass cytometry revealed the immunomodulatory effect of cisplatin via downregulation of splenic CD44+, IL-17A+ MDSCs and promotion of circulating IFN-gamma+ myeloid cells in the 4T1 metastatic breast cancer model. *Int J Mol Sci* 2019;21:170.
- [42] Tertilt C, Joh J, Krause A, Chou P, Schneeweiss K, Crystal RG, et al. Expression of B-cell activating factor enhances protective immunity of a vaccine against *Pseudomonas aeruginosa*. *Infect Immun* 2009;77:3044–55.
- [43] Kallert SM, Darbre S, Bonilla WV, Kreutzfeldt M, Page N, Muller P, et al. Replicating viral vector platform exploits alarmin signals for potent CD8+ T cell-mediated tumour immunotherapy. *Nat Commun* 2017;8:15327.
- [44] Papo M, Corneau A, Cohen-Aubart F, Robin B, Emile JF, Miyara M, et al. Immune phenotyping of Erdheim-Chester disease through mass cytometry highlights decreased proportion of non-classical monocytes and increased proportion of Th17 cells. *Ann Rheum Dis* 2020;79:1522–4.